10422 *Inorg. Chem.* **2010**, *49*, 10422–10426
DOI: 10.1021/ic101286j

Inorganic Chemistry
Article

An Unusual 3D Entangled Co(II) Coordination Polymer Directed by Ferromagnetic Molecular Building Block

Jian-Qiang Liu,[†,‡] Bin Liu,[†] Yao-Yu Wang,[*,†] Ping Liu,[†] Guo-Ping Yang,[†] Rui-Ting Liu,[†] Qi-Zhen Shi,[†] and Stuart R. Batten[§]

[†]*Key Laboratory of Synthetic and Natural Functional Molecule Chemistry of the Ministry of Education, Shaanxi Key Laboratory of Physico−Inorganic Chemistry, College of Chemistry & Materials Science, Northwest University, Xi'an 710069, P. R. China,* [‡]*Guangdong Medical College, School of Pharmacy, Dongguan, 523808, P. R. China, and* [§]*School of Chemistry, Monash University, Victoria 3800, Australia*

Received June 28, 2010

A fascinating 3D entangled metal−organic framework, namely, $\{[Co_2(bcp)_2]\cdot 3H_2O\}_n$ (**1**), was obtained through the solvothermal generation of flexible and long dicarboxylate (bcp) and metal salt. The crystal structure contains a 1D metal chain with bcp ligands wrapped around it in a wavy line and features an unusual entangled topological net. Furthermore, the magnetic behavior of **1** was also studied and indicated the existence of ferromagnetic interaction and long-range ordering character.

Introduction

The design and preparation of molecule-based magnets has attracted a great deal of attention, especially for the metal−organic systems involving magnetism of small clusters and chains with unconventional behaviors.[1] Up to now, a series of different dimensional (1D, 2D, and 3D) structure compounds based on Mn(II), Cu(II), and Ni(II) metal clusters have been obtained by bridging of N_3^-, ox, and $N(CN)^-$, showing behaviors from those of a single-molecule magnet to classical magnet and dynamic behaviors.[2,3] As is well-known, the magnetic strength and nature of the magnetic coupling between metal centers can be determined by the bridging linkers.[4] Carboxylate linkers have been widely employed to shape molecular magnetic materials owing to their various binding modes that afford superexchange pathways.[5] So far, the design and synthesis of polynuclear metal−carboxylate complexes and extended networks with predictable magnetic properties are still a challenge in the field of molecular magnetism. In particular, homometallic 3D metal−carboxylate motifs containing small metal chains give a chance for exploring the relationship between the structure and metamagnetic characters due to the possibilities of enhancement of the bulk magnetic interactions.[6]

1,3-Bis(4-carboxy-phenoxy)propane (H_2bcp) is an example of a long, V-shaped, and flexible dicarboxylate ligand, which has been employed by us to construct exceptional sextuple-stranded molecular braids in the presence of flexible bbp (1,3-bis(4-pyridyl)propane) ligands.[7] To design a homometallic metal−organic framework showing interesting magnetic behavior, we have used the Co(II) atom with large magnetic anisotropy and a single bridging bcp ligand, and we successfully obtained a 3D entangled polymer $\{[Co_2(bcp)_2]\cdot 3H_2O\}_n$ (**1**), which contains a 1D unusual metal chain and displays ferromagnetism.

*To whom correspondence should be addressed. E-mail: wyaoyu@nwu.edu.cn.

(1) (a) Kahn, O. *Molecular Magnetism*; VCH: New York, 1993. (b) Chen, X. N.; Xue, W.; Zhang, W. X.; Chen, X. M. *Chem. Mater.* **2008**, *20*, 5345. (c) Miller, J. S.; Epstein, A. J. *Angew. Chem., Int. Ed.* **1994**, *33*, 385. (d) Wang, S.; Zuo, J. L.; Gao, S.; Zhou, H. C.; You, Y. Z. *J. Am. Chem. Soc.* **2004**, *126*, 8900. (e) Gatteschi, D.; Sessoli, R. *Angew. Chem., Int. Ed.* **2003**, *43*, 268. (f) Coronado, E.; Dunbar, K. R. *Inorg. Chem.* **2009**, *48*, 3293. (g) Kahn, O. *Acc. Chem. Rev.* **2000**, *33*, 647. (h) Zeng, Y. F.; Hu, X.; Liu, F. C.; Bu, X. H. *Chem. Soc. Rev.* **2009**, *38*, 469. (i) Li, J. R.; Yu, Q.; Sañudo, E. C.; Tao, Y.; Bu, X. H. *Chem. Commun.* **2007**, 2602. (j) Zeng, Y. F.; Hu, X.; Zhao, J. P.; Hu, B. W.; Sañudo, E. C.; Liu, F. C.; Bu, X. H. *Chem.—Eur. J.* **2008**, *14*, 7127. (k) Murrie, M. *Chem. Soc. Rev.* **2010**, *39*, 1986.

(2) (a) Clérac, R.; Miyasaka, H.; Yamashita, M.; Coulon, C. *J. Am. Chem. Soc.* **2002**, *124*, 12837. (b) Kepert, C. J. *Chem. Commun* **2006**, 695. (c) Zhang, X. M.; Zhao, Y. F.; Zhang, W. X.; Chen, X. M. *Adv. Mater.* **2007**, *19*, 2843. (d) Humphrey, S. M.; Wood, P. T. *J. Am. Chem. Soc.* **2004**, *126*, 13236.

(3) (a) Gao, E. Q.; Yue, Y. F.; Bai, S. Q.; He, Z.; Yan, C. H. *J. Am. Chem. Soc.* **2004**, *126*, 1419. (b) Li, X. J.; Wang, X. Y.; Gao, S.; Cao, R. *Inorg. Chem.* **2006**, *45*, 1508. (c) Ishii, N.; Okamura, Y.; Chiba, S.; Nogami, T.; Ishida, T. *J. Am. Chem. Soc.* **2008**, *130*, 24. (d) Gao, E. Q.; Wang, Z. M.; Yan, C. H. *Chem. Commun* **2003**, 1748.

(4) (a) Zhou, Y. L.; Wu, M. C.; Zeng, M. H.; Liang, H. *Inorg. Chem.* **2009**, *48*, 1046. (b) Wang, X. Y.; Sevov, S. C. *Inorg. Chem.* **2008**, *47*, 1037. (c) Demessence, A.; Rogez, G.; Rabu, P. *Chem. Mater.* **2006**, *18*, 3005. (d) Huang, F. P.; Tian, J. L.; Gu, W.; Lin, X.; Yan, S. P.; Liao, D. Z.; Cheng, P. *Cryst. Growth Des.* **2010**, *10*, 1145. (e) Ribas, J.; Escuer, A.; Monfort, M.; Vicente, R.; Cortés, R.; Lezama, L.; Rojo, T. *Coord. Chem. Rev.* **1999**, *193*−*195*, 1027. (f) Gatteschi, D.; Sessoli, R. *Angew. Chem., Int. Ed.* **2003**, *42*, 268. (g) Sessoli, R.; Gatteschi, D.; Caneschi, A.; Novak, M. A. *Nature* **1993**, *365*, 141.

(5) (a) Kurmoo, M. *Chem. Soc. Rev.* **2009**, *38*, 1353. (b) Zeng, M . H.; Yao, M.; Liang, H. X.; Zhang, W. X.; Chen, X. M. *Angew. Chem., Int. Ed.* **2007**, *46*, 1832. (c) Zeng, M. H.; Zhang, W. X.; Sun, X. Z.; Chen, X. M. *Angew. Chem., Int. Ed.* **2005**, *44*, 3079.

(6) (a) Carlin, R. L. *Magnetochemistry*; Springer: Berlin, 1986. (b) Coronado, E.; Palacio, F.; Veciana, J. *Angew. Chem., Int. Ed.* **2003**, *115*, 2674.

(7) Liu, J. Q.; Wang, Y. Y.; Liu, P.; Dong, Z.; Shi, Q. Z.; Batten, S. R. *CrystEngComm* **2009**, *11*, 1207.

 Published on Web 10/14/2010

Table 1. Crystallographic Data and Structure Refinement Summary for Complex **1**

	1
formula	$C_{34}H_{33}Co_2O_{15}$
M_r	799.46
cryst syst	monoclinic
space group	$C2/c$
a (Å)	13.842(2)
b (Å)	24.652(4)
c (Å)	10.5305(17)
α (deg)	90
β (deg)	105.241(3)
γ (deg)	90
V (Å^3)	3467.0(9)
Z	4
F (000)	1644
D_{calcd} (g/cm^3)	1.532
GOF	1.036
reflns collected	3105
unique reflns	8609 (R_{int} = 0.0315)
final R indices	R_1 = 0.0504
R^{α} ($I > 2\sigma(I)$)	wR_2 = 0.1456
R indices[a,b]	R_1 = 0.0654
(all data)	wR_2 = 0.1555

[a] $R_1 = \sum||F_o| - |F_c||/\sum|F_o|$. [b] $wR_2 = \{\sum[w(F_o^2 - F_c^2)^2]/\sum(F_o^2)^2\}^{1/2}$.

Experimental Section

Materials and Instruments. All reagents were purchased from commercial sources and used as received. The IR spectrum was recorded with a Perkin−Elmer Spectrum One spectrometer in the region 4000−400 cm^{-1} using KBr pellets. TGA was carried out with a Mettler-Toledo TA 50 in dry dinitrogen (60 mL min^{-1}) at a heating rate of 5 °C min^{-1}. X-ray powder diffraction (XRPD) data were recorded on a Rigaku RU200 diffractometer at 60 kV and 300 mA using Cu Kα radiation (λ = 1.5406 Å), with a scan speed of 2 °C/min^{-1} and a step size of 0.02° in 2θ. Magnetic susceptibility data of powdered samples restrained in parafilm were measured on an Oxford Maglab 2000 magnetic measurement system in the temperature range 2−300 K and in a field of 1 kOe. Diamagnetic correction was applied using Pascal's constant.[8]

X-Ray Crystallography. Single-crystal X-ray diffraction analysis of the title compound was carried out on a Bruker SMART APEX II CCD diffractometer equipped with graphite monochromated Mo Kα radiation (λ = 0.71073 Å) by using the ϕ/ω scan technique at room temperature. The intensities were corrected for Lorentz and polarization effects as well as for empirical absorption based on multiscan techniques. The structure was solved using the direct method and refined by full-matrix least-squares fitting on F^2 by SHELX-97.[9] Absorption correction was applied by using the multiscan program SADABS.[10] The hydrogen atoms of the organic ligand were placed in calculated positions and refined using riding on attached atoms with isotropic thermal parameters 1.2 times those of their carrier atoms. The water hydrogen atoms were located from difference maps and refined with isotropic thermal parameters 1.5 times those of their carrier atoms. Table 1 shows crystallographic data of **1**. Selected bond distances and bond angles are listed in Table 2.

Synthesis. Preparation of $\{[Co_2(bcp)_2]\cdot 3H_2O\}_n$ (1). A mixture of $Co(NO_3)_2\cdot 3H_2O$ (0.025 g, 0.11 mmol), 1,3-bis(4-carboxy-phenoxy)propane (H_2bcp) (0.032 g, 0.1 mmol), CH_3OH (2 mL), CH_3CN (1 mL), and NaOH (0.5 M, 0.4 mL) and deionized water (8 mL) was stirred for 30 min in the air, then transferred and sealed in a 25 mL Teflon reactor, which was heated at 150 °C for 72 h. The solution was then cooled to room temperature at a rate of 5 °C h^{-1}, to yield a very fine pink crystalline product (**1**) in 40% yield (based on Co). $C_{34}H_{33}Co_2O_{15}$ (799.46) (**1**) Anal. Calcd: C, 51.18; H, 4.16. Found: C, 52.33; H, 3.88. IR (cm^{-1}): 3419vs, 3022m, 1554s, 1405s, 1249 m, 781 m.

Table 2. Selected Bond Distances (Å) and Angles (deg)[a]

complex **1**			
Co(1)−O(6)#1	2.012(3)	Co(2)−O(3)#2	2.074(2)
Co(1)−O(4)#3	2.085(2)	Co(2)−O(4)#4	2.302(2)
Co(2)−O(5)#5	2.200(2)		
O(6)−Co(1)−O(6)	102.42(17)	O(4)−Co(1)−O(4)	101.05(12)
O(6)−Co(1)−O(4)	110.41(11)	O(3)−Co(2)−O(3)	180.0
O(5)−Co(2)−O(5)	180.0	O(4)−Co(2)−O(4)	180.0

[a] Symmetry codes. #1: $-x, y, 3/2 - z$; #2: $-x, 1 - y, 1 - z$; #3: $1/2 + x, 1/2 + y; 1 + z$; #4: $-1/2 - x, 1/2 + y; 1/2 - z$; #5: $-1/2 - x, 1/2 - y, -z$.

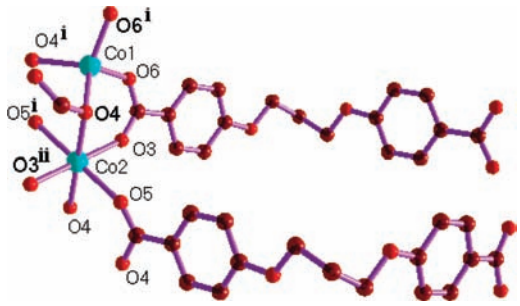

Figure 1. Coordination environment of Co(II) center and coordination mode of bcp ligand (symmetric codes: (i) $x - 1/2, y + 1/2, z - 1$; (ii) $-x + 2, -y + 1, -z$).

Results and Discussion

X-ray analysis reveals that the asymmetric unit of **1** contains one Co(II) atom (both Co1 and Co2 have 1/2 site occupancies), one bcp ligand, and one-half of a lattice water molecule. The bcp exhibits a $(K^1-K^1)-(K^1-\mu_2)-\mu_5$ bridging mode.[11] The Co1 center adopts a distorted tetrahedral CoO_4 coordination environment provided by four oxygen atoms from two symmetric bridging carboxylate groups (two oxygen atoms come from (K^1-K^1) ends, and the remaining sets originate from μ_2-bridging groups), while the Co2 shows a normally octahedral CoO6 coordination environment derived from two (K^1-K^1) and four $(K^1-\mu_2)$ bridging ends (Figure 1). The Co−O distances agreed with the normal values in reported polymers.[4a,7] In **1**, on the basis of this connection, it extends along the crystallographic *a* axis *via* bridging carboxylates, generating an infinite metal chain through sharing Co(II) ions, as shown in Figure 2. The chain presents a wave-like motif. The intrachain Co(II)···Co(II) distance and Co1−O−Co2 angle are 3.332(1) Å and 98.71(8)°, respectively. In the literature, several notable MOFs built on $Co_2(\mu_2\text{-}OH_2)(CO_2)_4$ [the binuclear core exhibits the (μ-aqua)bis(μ-carboxylate) unit], $Co_4(\mu_3\text{-}OH)(CO_2)_6$ [the four cobalt atoms form a tetranuclear unit through bodings from two bridging μ_3-OH and carboxylate groups], and $Co_7(\mu_3\text{-}OH)_2$-(bhqe)$_6$ [Co1 is coordinated by six μ_3-alkoxo oxygen atoms from three bhqe ligands, while six symmetry equivalent Co2 atoms are arranged in a staggered fashion, three up and three down along the *c* axis, sandwiching the Co1] molecular building blocks (MMBs) have been documented,[12] but there is no an instance

(8) Carlin, R. L. *Magnetochemistry*; Spring-Verlag: Berlin, 1986; p 3.
(9) Sheldrick, G. M. *SHELXL-97*; University of Göttingen: Göttingen, Germany, 1997.
(10) Sheldrick, G. M. *SADABS 2.05*; University of Göttingen: Göttingen, Germany, 2002.
(11) Lian, F. Y.; Jiang, F. L.; Yuan, D. Q.; Chen, J. T.; Wu, M. Y.; Hong, M. C. *CrystEngComm* **2008**, *10*, 905.
(12) (a) Chen, Q.; Zeng, M. H.; Zhou, Y. L; Zou, H. H.; Kurmoo, M. *Chem. Mater.* **2010**, *22*, 2114. (b) Cañadillas-Delgado, L.; Fabelo, O.; Pasán, J.; Delgado, F. S.; Lloret, F.; Julve, M.; Ruiz-Pérez, C. *Inorg. Chem.* **2007**, *46*, 7458. (c) Lama, P.; Aijaz, A.; Sañudo, E. C; Bharadwaj, P. K. *Cryst. Growth Des.* **2010**, *10*, 283.

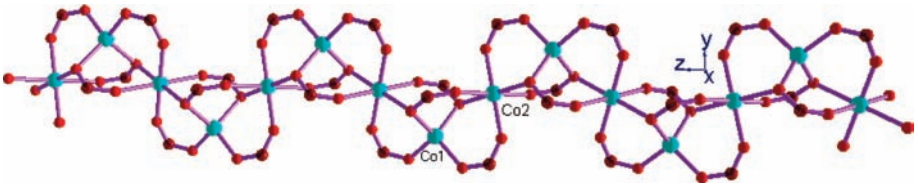

Figure 2. The unusual 1D metal chain showing wave-like fashion.

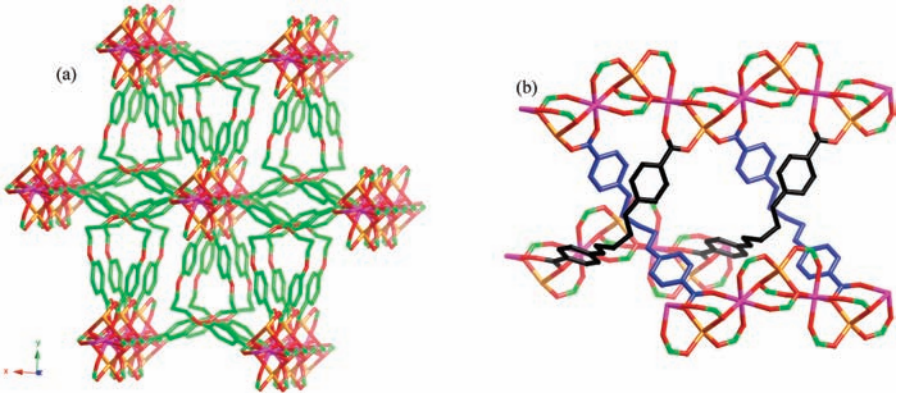

Figure 3. (a) The cross-linking of 1D metal−carboxylate chains by the bcp ligands to give an overall 3D structure for compound **1**. For clarity, the two crystallographically unique metal atoms are colored differently (orange and purple). (b) The unusual fashion in which pairs of ligands bend around each other in the structure of **1**.

built on this special molecular building block. Thus, it believed that the present $Co_2(CO_2)_4$ MMB is unique and unprecedented. These chains are then connected to each other *via* the bcp ligands, to give an overall 3D network (Figure 3a). Each chain connects to six others, with each pair of chains connected to two sets of bcp ligands. Interestingly, the V-shaped conformation adopted by the bcp ligand leads to them wrapping around each other in an unusual fashion, as shown in Figure 3b. To the best of our knowledge, such a wrapping fashion character is quite rare. Most known structures of lanthanide and transition-metal compounds are double- or triple-stranded helicates directed by long polydentate linkers.[13] These flexible linkers are able to wrap around metal atoms forming compact helical structures. The example is described by an interweaving of single and novel unequal double-helical chains formed by complicated linkages of the tripodal ligands and flexible N-donor ligands between different Ni(II) centers.[13b]

Another structural feature of **1** is the presence of two kinds of helical chains within one sheet (Figure 4). The Co1 ions are connected by bcp ligands, leading to a 2D sheet containing left- and right-handed helices, while the Co2 ions are linked by bcp to form a 1D double chain, as shown in Figure S1 (Supporting Information). From the perspective view, the helix-like subunits construct a beautiful hexagonal diagram. The lattice water molecules are shaped like trimer water clusters and are filled in the cavity.

The temperature-dependent molar magnetic susceptibility of **1** was measured at 1000 Oe in the range 2−300 K on a polycrystalline powder sample (Figure 5). At room temperature, $\chi_M T$ is 3.28 $cm^3\ mol^{-1}$ K, which is larger than the spin-only value (1.875 $cm^3\ mol^{-1}$ K) for $S = 3/2$, indicating the important orbital contribution arising from the high-spin octahedral Co(II).[14] $\chi_M{}^{-1}$ obeys the Curie−Weiss law with a Curie constant of 3.22 cm^3 K mol^{-1} and a Weiss constant of $\theta = +6.14$ K. The positive θ value is indicative of a dominant ferromagnetic interaction between Co^{2+} centers.[1a] Upon cooling, the $\chi_M T$ value is almost constant from 3.28 cm^3 K mol^{-1} at 300 K to 3.78 cm^3 K mol^{-1} at 50 K and then increases drastically to a maximum of 20.42 $cm^3\ mol^{-1}$ around 3.0 K, suggesting an appreciable intrachain ferromagnetic exchange between Co1 and Co2 connected to each other through μ_2-O and O−C−O bridges. The sudden decrease in $\chi_M T$ below 3.0 K may be attributed to low-temperature magnetization saturation, and the interchain antiferromagnetic interaction and/or the zero-field splitting effect cannot be excluded.[15] The magnetic data above 3 K can be fitted using the equation derived by Fisher for a uniform chain of classical spins based on the Hamiltonian $\hat{H} = -2J\Sigma S_i S_{i+1}$, and the ise of this led to the parameters $J = 2.33\ cm^{-1}$ and $g = 2.64$ (see the Supporting Information).[16] Accounting for the interchain interactions zJ, the least-squares analysis of magnetic susceptibilities data led to the parameters $J = 2.66\ cm^{-1}$, $g = 2.60$, and $zJ = -0.024$ (Figure S2, Supporting Information).

In order to estimate the strength of the ferromagnetic exchange interaction and the spin−orbit coupling for the $^4T_{1g}$ state of Co^{2+}, the best fits above 30 K based on the equation listed in ref 17 gave the parameters $\lambda = -112\ cm^{-1}$,

(13) (a) Ghosh, S. K.; Bharadwaj, P. K. *Inorg. Chem.* **2004**, *43*, 2293. (b) Wang, S. N.; Xing, H.; Li, Y. Z.; Bai, J. F.; Scheer, M.; Pan, Y.; You, X. Z. *Chem. Commun.* **2007**, 2293.

(14) (a) Duan, Z. M.; Zhang, Y.; Zhang, B.; Zhu, D. B. *Inorg. Chem.* **2008**, *47*, 9152. (b) Coronado, E.; Galan-Mascaros, J. R.; Marti-Gastaldo, C.; Martinez, A. M. *Dalton Trans.* **2006**, 3294. (c) Calvo-Pérez, V.; Ostrovsky, S.; Vega, A.; Pelikan, J.; Spodine, E.; Haase, W. *Inorg. Chem.* **2006**, *45*, 644. (d) Humphrey, S. M.; Wood, P. T. *J. Am. Chem. Soc.* **2004**, *126*, 13236. (e) Konar, S.; Mukherjee, P. S.; Drew, M. G. B.; Ribas, J.; Chaudhuri, N. R. *Inorg. Chem.* **2003**, *42*, 2545.

(15) (a) Li, X. J.; Wang, X. Y.; Gao, S.; Cao, R. *Inorg. Chem.* **2006**, *45*, 1508. (b) Rittenberg, D. K.; Sugiura, K.; Sakata, Y.; Mikami, S.; Epstein, A. J.; Miller, J. S. *Adv. Mater.* **2000**, *12*, 126.

(16) Fisher, M. E. *Am. J. Phys* **1964**, *32*, 343.

(17) Raebiger, J. W.; Manson, J. L.; Sommer, R. D.; Geiser, U.; Rheingold, A. L.; Miller, J. S. *Inorg. Chem.* **2001**, *40*, 2578.

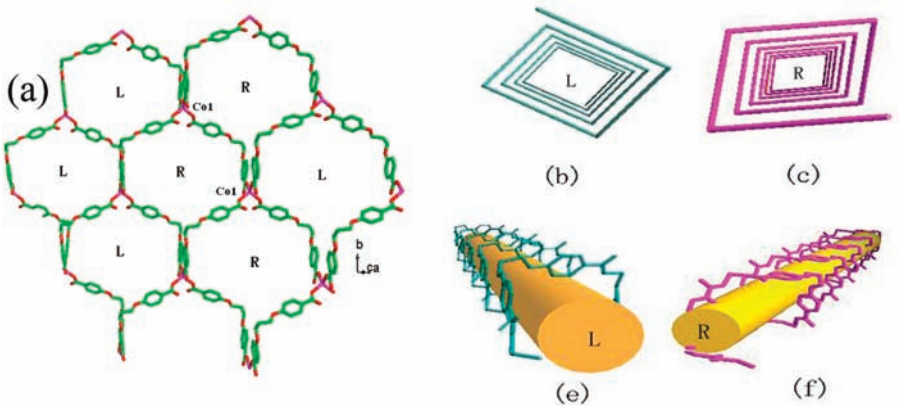

Figure 4. (a) The 2D layer directed by Co1 and bcp ligands. (b−f) the left- and right-handed helical tubues.

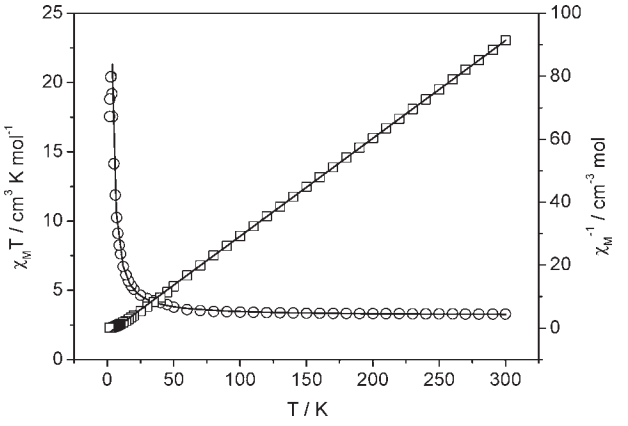

Figure 5. Plots $\chi_M T$ and $\chi_M{}^{-1}$ of versus T for **1**. Solid lines represent fits to the data (see text for details).

$A = 1.26$, and $\theta = 17.0$ K (Figure S3, Supporting Information). The data were fitted using the simple phenomenological equation (see the Supporting Information).[18] The least-squares analysis, shown as solid lines in Figure S4 (Supporting Information), led to parameters $A = 0.23$ cm^3 K mol^{-1}, $E_1/k = 84$ K, $B = 2.98$ cm^3 K mol^{-1}, and $E_2/k = -11.5$ K. Here, $A + B$ equals the Curie constant, the value for E_1/k is consistent with those given in the literature for the effects of both spin−orbit coupling and site distortion, and the value $E_2/k \propto -2J$, corresponding to spin coupling between Co^{2+} ions, shows the distinct ferromagnetic exchange mediated between Co^{2+} through μ_2-O and O−C−O bridges. The intrachain Co···Co distance and Co1−O−Co2 angle are 3.332(1) Å and 98.71(8)°, respectively. However, the shortest interchain Co···Co distance is 11.153(1) Å. This is in agreement with magnetostructural analysis: Co−Co ferromagnetic coupling due to small Co−O−Co and antiferromagnetic coupling due to large Co−O−Co angles.[19]

At a low applied field of 50 Oe in the temperature range 1.8−6 K, the magnetizations after zero field cooling (ZFC) and subsequent field cooling (FC) reveal nonreversibility and

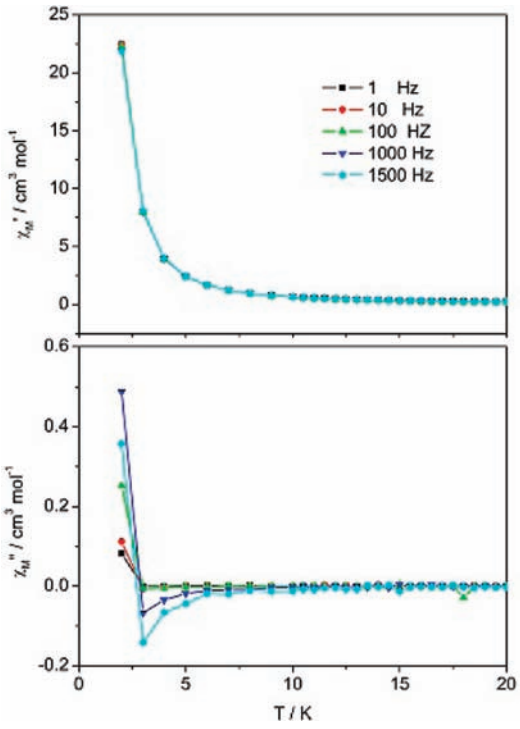

Figure 6. In-phase and out-of-phase component of the ac magnetic susceptibility data for **1**, recorded with switching frequencies of 1, 10, 100, 1000, and 1500 Hz.

bifurcation (Figure S5, Supporting Information), showing that long-range ordering occurs at 2.0 K. The temperature-dependent zero field ac susceptibility is measured under $H_{ac} = 3.5$ Oe and frequencies of 1, 10, 100, 1000, and 1500 Hz. Figure 5 clearly shows that the in-phase χ' and out-of-phase χ'' signals increase drastically around 2.0 K close to the T_c. The invariance of χ' and χ'' with the cycling frequency confirms that the material is not a spin glass.[13a,20] Obviously, the χ'' intensity enhances upon an increase in frequency; however, we estimate that the χ'' maximum position is independent of frequency. When the frequency enhances, the χ'' value drops to negative and then increases again below 2.0 K (Figure 6). Such magnetic behavior could be related to the measure sample without pressing consistency. The mechanism is, however, not clear to us. Magnetization (M) measurements on **1** (Figure 7) show a

(18) (a) Rueff, J. M.; Masciocchi, N.; Rabu, P.; Sironi, A.; Skoulios, A. *Eur. J. Inorg. Chem.* **2001**, 2843. (b) Rabu, P.; Rueff, J. M.; Huang, Z. L.; Angelov, S.; Souletie, J.; Drillon, M. *Polyhedron* **2001**, *20*, 1677. (c) Rueff, J. M.; Masciocchi, N.; Rabu, P.; Sironi, A.; Skoulios, A. *Chem.—Eur. J.* **2002**, *8*, 1813.

(19) (a) Salah, M. B.; Vilminot, S.; Andre, G.; Richard-Plouet, M.; Mhiri, T.; Takagi, S.; Kurmoo, M. *J. Am. Chem. Soc.* **2006**, *128*, 7972. (b) Rujiwatra, A.; Kepert, C. J.; Rosseinsky, M. *Chem. Commun.* **1999**, 2307. (c) Zhang, X. M.; Zhang, X. H.; Wu, H. S.; Tong, M. L.; Ng, S. W. *Inorg. Chem.* **2008**, *47*, 7462.

(20) Marino, N.; Mastropietro, T. F.; Armentano, D.; De Munno, G.; Doyle, R. P.; Lloret, F.; Julve, M. *Dalton Trans* **2008**, 5152.

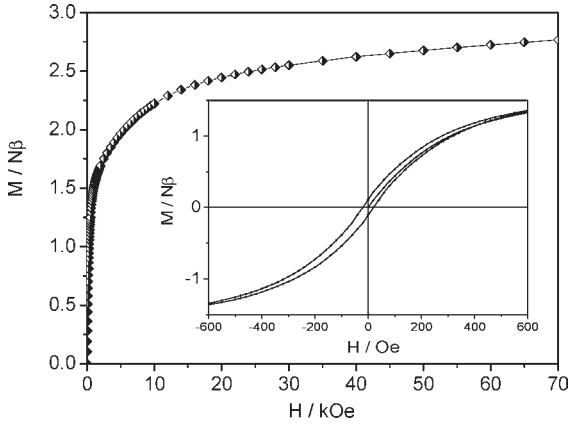

Figure 7. Magnetization of **1** as a function of magnetic field at 1.8 K.

rapid increase in M as a function of field (H), with M registering a value of 1.50 Nβ at H = 1 kOe (at 1.8 K). M continues to rise gradually thereafter, reaching 2.77 Nβ at H = 70 kOe. This behavior is consistent with a ferromagnetically ordered state of Co^{2+} for which the saturation magnetization would be in the range of 1.0−3.0 Nβ, attributed to the spin−orbital coupling. The magnetization versus field dependence at 2 K shows obviously hysteretic behavior. The remanent magnetization M_r is 0.11 Nβ, and the coercive field H_c is 20 Oe.

Compound **1** has stability in the air and retains its crystalline integrity under ambient conditions. Thermogravimetric analysis of compound **1** shows a loss of the lattice water molecules (5.5%) within the temperature range of 43−200 °C (calcd. 6.0%; Figure S6, Supporting Information). A further weight loss of 72.8% was observed in the range of 230−550 °C, which is in agreement with the removal of the bcp ligands. The result indicates that the new type of MMB network is thermally stable below these temperatures. Additionally, to confirm the phase purity and stability of compound **1**, the original sample and the dehydrated sample were both characterized by X-ray powder diffraction (XRPD) at room temperature. The pattern that was simulated from the single-crystal X-ray data of compound **1** was in good agreement with those that were observed (Figure S7, Supporting Information), indicating that compound **1** was obtained as a single phase. For compound **1**, after heating at 200 °C for 4 h, the guest water molecules were removed (the evacuated framework is defined as **1′**). The XRPD pattern of **1′** is similar to that of compound **1**, although minor differences can be seen in the positions, intensities, and widths of some peaks, which indicates that the framework of compound **1** is retained after the removal of the guest molecules.

Conclusions

In summary, an unusual 3D entangled metal−organic framework has been structurally and magnetically characterized. Structural analysis indicates that the assistant nuetral ligand would markedly control the resulting motifs on the basis of our previous example.[7] The compound shows ferromagnetic behavior and long-range ordering character.

Acknowledgment. We gratefully acknowledge financial support of this work by the National Natural Science Foundation of China (Grant No. 20771090), State Key Program of National Natural Science of China (Grant No. 20931005), Natural Science Foundation of Shaanxi Province (Grant No. 2009JZ001), and Specialized Research Foundation for the Doctoral Program of Higher Education (Grant No. 20096101110005).

Supporting Information Available: Fitted equations of magnetism, additional structural figures, magnetic figures, and the results of TGA and XRD. This material is available free of charge via the Internet at http://pubs.acs.org.